Available online at www.sciencedirect.com

SciVerse ScienceDirect

Ceramics International 39 (2013) 5281–5286

CERAMICS INTERNATIONAL

www.elsevier.com/locate/ceramint

Synthesis and optical limiting effects in ZrO_2 and $ZrO_2@SiO_2$ core–shell nanostructures

K. Mani Rahulan[a,*], G. Vinitha[b], L. Devaraj Stephen[a], Charles Christopher Kanakam[a]

[a]*Department of Chemistry, SRM Valliammai Engineering College, Kattankulathur, Chennai, India*
[b]*Department of Physics, VIT University, Chennai, India*

Received 15 October 2012; received in revised form 30 November 2012; accepted 9 December 2012
Available online 20 December 2012

Abstract

ZrO_2 nanoparticles were synthesized by the chemical precipitation method and coated with silica through seeded polymerization technique to form core–shell type $ZrO_2@SiO_2$ nanostructures. The structural, morphological and silica coating formation of the bare and silica coated particles were studied using Transmission electron microscopy, X-ray diffraction and Fourier Transform Infrared Spectroscopy. Thermogravimetric analysis and Zeta potential measurements were performed to check the thermal and dispersion stability of the nanostructures. The optical limiting performance of these nanostructures was studied using open-aperture Z-scan technique in which nanosecond laser pulses at 532 nm have been used for optical excitation. Both bare and silica coated ZrO_2 nanoparticles exhibited good optical limiting behavior due to excited state absorption, arising from effective three photon absorption. It is observed that the optical nonlinearity is enhanced in core shell structures as compared with the bare particles.

Keywords: Core–shell nanoparticles; Stober method; X-ray diffraction; Optical limiting

1. Introduction

Zirconia (ZrO_2) nanoparticles have attracted much interest due to their enhanced optical and electrical properties with applications as piezoelectric, electro-optic and dielectric material [1]. Because of their obvious improvement in hardness, wear resistance, and thermal shock resistance, ZrO_2 has turned into a technologically promising ceramic material of the current generation. The approach for designing and fabricating such material in a core–shell model has attracted considerable attention because these nanoparticles with a well defined core and shell structures often exhibit improved physical and chemical properties over their single component counterparts. A variety of methods have been demonstrated for the preparation of nanoparticles in a core–shell model during the past decades. Some investigators reported that such particles could be prepared by encapsulation of inorganic particles in a polymer shell [2,3]. Mohamed El-Toni et al. reported novel silica coating of titania nanoparticles by seeded polymerization technique with optimization of coating parameters to obtain a dense silica coating for titania nanoparticles [4]. The formation of silica coating layers on ZrO_2 is important in a broader range of applications. The uniformly coated shell provides enhancement to the core along with passivation and extra functionalities. An appropriate shell layer can protect the core metal from the damage of high energy laser pulses, improve resistance to possible chemical reactions of the metal with its environment and even modify the electrical and optical properties of nanoparticles.

In this study, core–shell type ZrO_2 and $ZrO_2@SiO_2$ nanoparticles were synthesized through the combination of chemical precipitation method and seeded polymerization approach. The structural and morphology of these nanocomposites were characterized by using various advanced techniques such as transmission electron microscopy (TEM) and X-ray diffractometer (XRD). The interactions and framework substitution between core and shell components are then measured by using Fourier transform

*Corresponding author. Tel./fax: +91 97 91012149.
E-mail addresses: krahul.au@gmail.com (K. Mani Rahulan), charlesckin@yahoo.com (C.C. Kanakam).

0272-8842/$ - see front matter © 2012 Elsevier Ltd and Techna Group S.r.l. All rights reserved.
http://dx.doi.org/10.1016/j.ceramint.2012.12.029

infrared spectroscopy (FTIR). The Nonlinear optical limiting performance of bare and core–shell nanoparticles was studied by open aperture Z-scan measurement using 7 ns Nd-YAG laser pulses at 532 nm.

2. Experimental section

2.1. Chemicals

Special grade reagents zirconium chloride hectahydrate $ZrCl_2O \cdot 8H_2O$ (Aldrich Chemicals Ltd., USA), Tetraethylorthosilicate (TEOS) (Sigma Chemicals, USA), Ethanol (SISCO Research Laboratories, India) were used for silica coating and ammonia (25% aqueous solution) was used as catalyst. All other chemicals were reagent grade and used without further purification. Ultrapure deionized water was used in all the preparations.

2.2. NLO properties measurements:

Optical limiting properties were investigated from open aperture Z-Scan experiments with 7 ns laser pulses at 532 nm from a frequency doubled, Q switched Nd:YAG laser. Samples were prepared by dispersing the nanoparticles in ethylene glycol and the solution was taken in a 1 mm cuvette. The spatial profile of the pulsed beam was nearly of Gaussian form after spatial filtering. The pulsed beam was split into two parts: the reflected part was used as reference, and the transmitted part was focused onto samples by using a 20 cm focal length lens. The beam's propagation direction is taken as the z-axis, and the focal point is taken as $z=0$. On approaching the focus the intensity increases by several orders of magnitude relative to the intensity away from focus, inducing nonlinear absorption in the sample. Laser pulses were fired at a repetition rate of 1 Hz, and the data acquisition was automated. The pulse energy reaching the sample was approximately 150 μJ.

2.3. Synthesis of ZrO_2 nanoparticles

Initially, NH_4OH dissolved in 200 ml of distilled water was taken in a beaker and pH was adjusted to 10.5. After maintaining the pH to 10.5, $ZrCl_2O \cdot 8H_2O$ of 0.1 mol/L was added dropwise to NH_4OH solution under vigorous stirring. The resultant particles were washed by repeated cycles of centrifugation. Washing was performed for a minimum of three times in ethanol. The obtained nanoparticles were kept in oven at 100 °C for 12 h followed by calcination at 400 °C for 2 h. Finally, the sample was crushed into fine powder.

2.4. Coating of silica on ZrO_2 nanoparticles

Silica-coating was done by means of seeded polymerization technique based on the Stober process [5] to encapsulate ZrO_2 nanoparticles. Initially, ZrO_2 nanoparticles were dispersed in ethanol by sonication at a concentration of 3 g/L for 10 min and then predetermined amount of tetraethylorthosilicate (TEOS) was added to the above suspension to carry out the silica growth. The ZrO_2/TEOS was allowed to stir for 30 min, thereafter ammonium hydroxide was added in a 1:4 TEOS to NH_4OH volume ratio. The mixture was stirred for 24 h to ensure completion of the reaction. Finally, the obtained precipitate was separated by centrifugation and washed with ethanol to remove the secondary silica particles.

2.5. Optical absorption

UV–vis absorption spectrum of ZrO_2 and ZrO_2@SiO_2 nanoparticles is shown in Fig. 1. It is seen that the absorption band edge corresponding to the nanocomposites gets significantly red shifted for silica capped ZrO_2. The reason for such absorption band may be attributed to the absorption by the silica nanoparticles, adsorbed on the surface of ZrO_2 particles. The position of the peak is not sensitive to the change in coating thickness, but its intensity is increased due to formation of silica shells. The shift in the absorption band toward longer wavelength indicates increase in particle diameter.

2.6. Transmission electron microscope (TEM)

The morphology of the synthesized nanoparticles is analyzed by TEM technique. It can be seen from Fig. 2 that the composite material is partly composed of clusters containing composite nanoparticles adhering to each other. From the picture, the particle size distribution of ZrO_2 @SiO_2 nanoparticles were found to be around 35 nm. Due to the electron density differences, the ZrO_2 and silica particles appeared to be darker and lighter parts, respectively. However, some core-free silica particles were also observed. This is probably due to a decrease in ionic strength of the

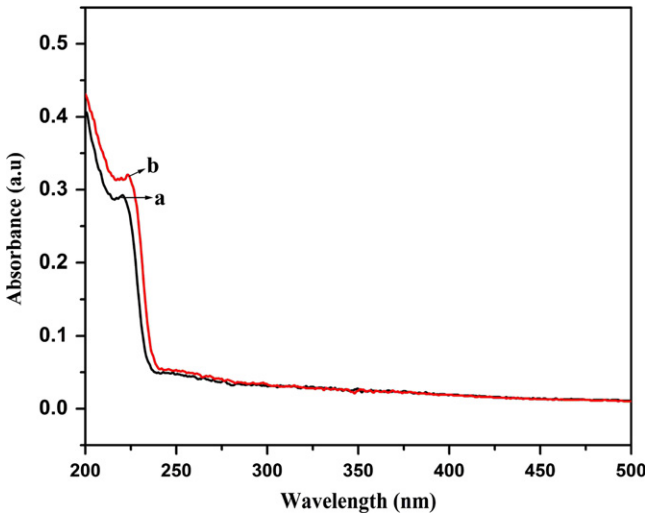

Fig. 1. UV–vis absorption spectra of: (a) ZrO_2 and (b) Silica coated ZrO_2 nanoparticles.

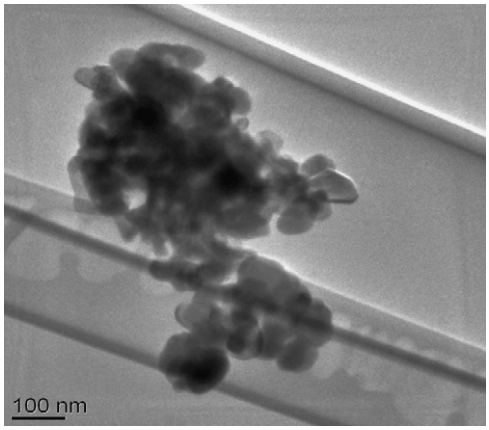

Fig. 2. TEM picture of silica coated ZrO_2 nanoparticles.

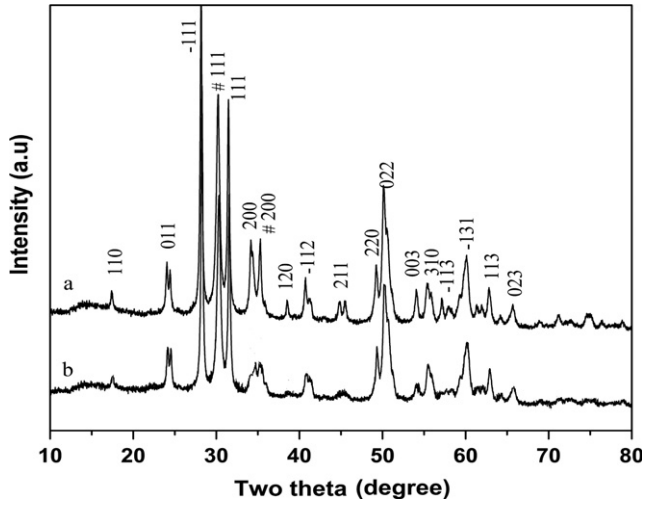

Fig. 3. XRD patterns of: (a) ZrO_2 and (b) silica coated ZrO_2 nanoparticles.

solution and the resulting increase in electrostatic repulsion between the core particle and silica nuclei.

2.7. X-ray diffraction (XRD)

The crystalline phase and purity of ZrO_2 were characterized by XRD. Fig. 3 shows the XRD pattern of the as-synthesized and silica coated zirconia nanoparticles. It can be seen that pure ZrO_2 exhibits good crystallinity and is predominantly in the monoclinic phase, with a small fraction in the tetragonal phase. The diffraction patterns of the monoclinic phase of ZrO_2 nanoparticles coincide with the standard data of (JCPDS-37-1484) with lattice parameters $a=5.3125$ Å, $b=5.2125$ Å and $c=5.1477$ Å. The diffraction patterns of the tetragonal phase are in good agreement with the standard data of (JCPDS-17-0923). For silica coated ZrO_2 nanoparticles, some of the peaks for ZrO_2 are not clearly seen due to dense silica coating on its surface.

2.8. FT-IR spectra

The FT-IR spectra of pure and silica encapsulated ZrO_2 nanoparticles are shown in Fig. 4. The O–H stretching vibration of free water between 3200 and 3700 cm^{-1} and its corresponding O–H bending vibration at 1636 cm^{-1} due to the chemically adsorbed water [6] were detected for both bare and silica coated ZrO_2 nanoparticles. The peaks at 1000–1250 cm^{-1} corresponds to the asymmetric vibration of Si–O–Si. The band at around 967 cm^{-1} is assigned to the stretching vibration modes of Zr–O–Si groups [7]. All these features indicate the formation of heterogeneous Si–O–Zr bonds at the interface of SiO_2–ZrO_2 in the prepared samples.

2.9. Thermogravimetric analysis

Results of thermogravimetric analysis (TGA) of the both as-pepared and silica capped ZrO_2 nanoparticles are shown in Fig. 5. Here both particles show weight losses in

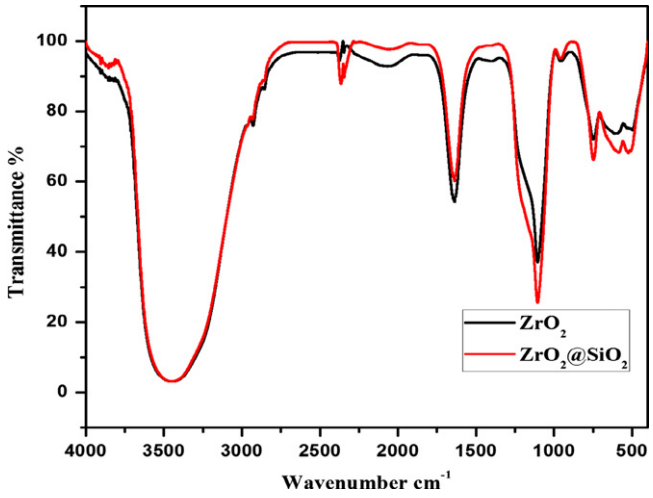

Fig. 4. FTIR of (a) ZrO_2 and (b) silica coated ZrO_2 nanoparticles.

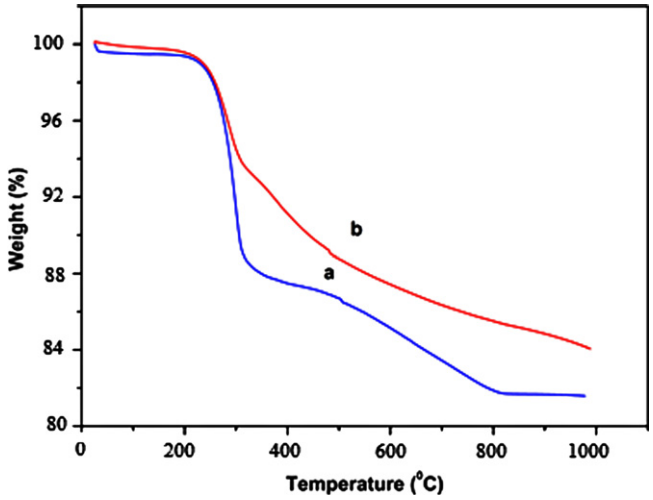

Fig. 5. TGA curves of: (a) ZrO_2 and (b) silica coated ZrO_2 nanoparticles.

three steps. The total weight loss is between room temperature and 800 °C. The first weight loss is in the temperature range 30–152 °C; this weight loss is attributed to evaporation of water from the layers of ZrO_2. The second weight loss is between the temperature range of 245–355 °C; the third weight loss is in the temperature range 355–800 °C. The second and third weight losses are attributed to decomposition of silanol groups and evaporation of structurally bound water.

2.10. Atomic force microscopy (AFM)

AFM images as depicted in Fig. 6 reveal the nanotopography of ZrO_2 nanoparticles coated with silica. In the AFM picture, the surface appears to be rugged due to the coating of silica on the ZrO_2 nanoparticles

2.11. Zeta potential measurements

Stability of the nanoparticles is crucially important for many applications. The dispersion stability of the particles is characterized with zeta potential measurements. Fig. 7 shows zeta potential distributions of bare and core–shell nanoparticles dispersed in water. Zeta potential is the net surface charge of the nanoparticles when they are inside a solution. The fact that particles push each other and their agglomeration behavior depends on large negative or positive zeta potential. To believe the particles as stable,

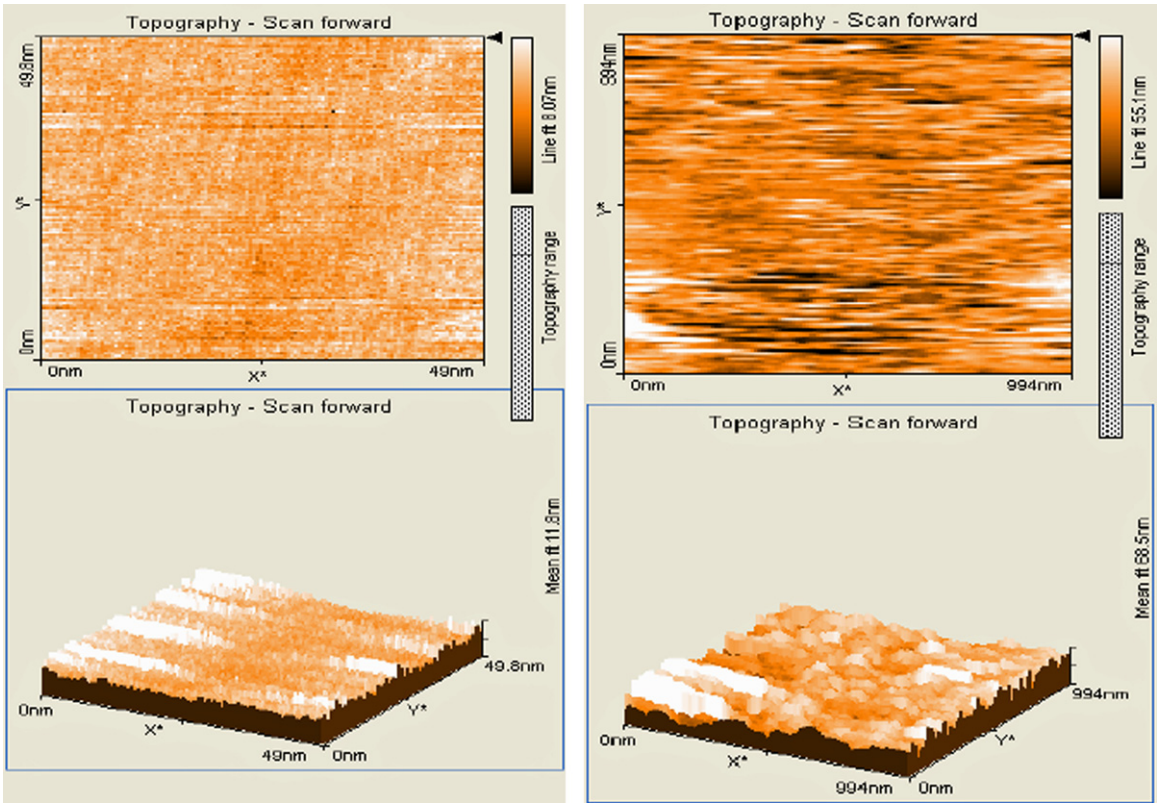

Fig. 6. AFM images of silica coated ZrO_2 particles.

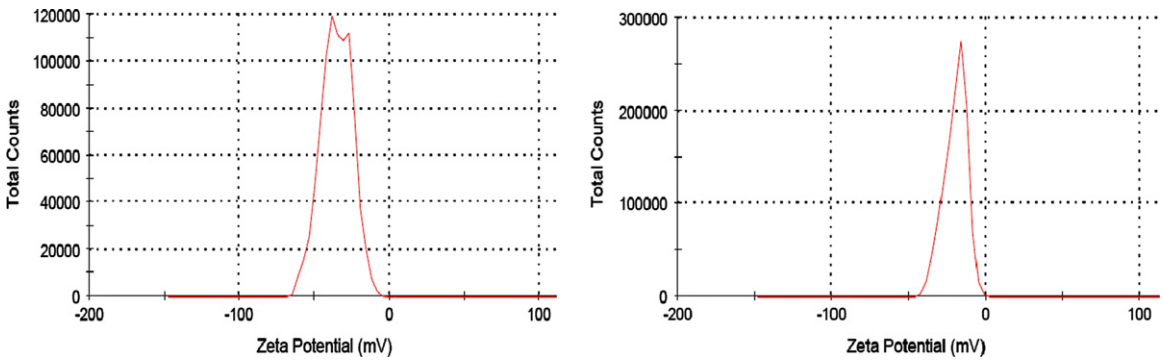

Fig. 7. Zeta potential distributions of: (a) ZrO_2 and (b) silica coated ZrO_2 nanoparticles.

zeta potential should either be higher than +30 mV or lower than −30 mV [8]. It is noted that the measured zeta potential varies between −35.2 mV and −19.8 mV for ZrO_2 and ZrO_2@SiO_2 nanostructures, respectively. The zeta potential values of silica coated nanoparticles are greater than the bare nanoparticles. This demonstrates that repulsion force is stronger in silica coated nanoparticles than the bare nanoparticles. The silica coated particles are therefore having good dispersion stability in aqueous solution.

3. Optical limiting measurements

The open-aperture Z-scan (i.e. without aperture in front of the detector) is performed to measure the magnitude of the nonlinear absorption coefficient of the nanopar ticles. Fig. 8 shows the open aperture Z-scans obtained for both ZrO_2 and silica encapsulated nanoparticles. The curve exhibits a normalized transmittance valley, indicating the presence of induced absorption in the colloids. Interestingly the nonlinear transmissions are found to be effectively of fifth order as it fits to a three-photon absorption (3 PA) processes. 3 PA cannot easily be identified from either the Z-scan technique or an optical limiting experiment. One has to utilize the photophysical properties of a material, e.g., linear absorption, 3 PA cross section, etc., to determine the contribution of multi-photon absorption. Once the multi-photon processes are confirmed, one can obtain some important parameters of materials by fitting the Z-scan or optical limiting data using appropriate theoretical models [9]. Therefore, the intensity versus normalized transmission curves derived from the Z-scan data are numerically fitted to the nonlinear transmission equation which gives best fit for a 3 PA process.

The normalized transmittance in the case of the open aperture scheme can be determined as

$$T = \frac{(1-R)^2 \exp(-\alpha L)}{\sqrt{\pi} p_0} \int_{-\infty}^{+\infty} \ln\left[\sqrt{1+p_0^2}\exp\left(-2t^2\right) + p_0 \exp\left(-t^2\right)\right] dt$$

where R is the surface reflectivity and p_0 is given by $2\gamma(1-R)^2 I_0^2 L$, where γ is the three photon absorption coefficient, L is the sample length and I_0 is the on-axis peak intensity. α is the linear absorption coefficient. From the best fits, the three-photon absorption coefficients are extracted and plotted. Different processes, such as 2 PA, multiphoton absorption, free carrier absorption, transient absorption, interband absorption, photoejection of electrons, and nonlinear scattering, are reported to be operative in nanoclusters. It is important to note the size and shape of nanoparticle when one considers the nonlinear optical processes in nanoparticle-containing suspensions, since the influence of quantum confinement on the nonlinear optical properties of the medium strongly depends on the spatial characteristics of the nanoparticles. The nonlinear absorption coefficients (γ) for ZrO_2 and ZrO_2 @SiO_2 are 0.9×10^{-23} m^3/W^2 and 1.1×10^{-23} m^3/W^2, respectively. It is seen that optical limiters based on silica coated particles possess better limiting characteristics as compared to their single counter parts. It is reported that the nonlinear absorption coefficient increases in the core–shell silica nanocomposites as compared to pure nanoparticles [10]

Nonlinear optical properties of semiconductor nanostructures depend mainly on their size and the excitation wavelength. Factors such as nature of the surface of the nanocluster, particle size and the distribution of particles, influence the response to a great extent. The interaction between the core and the shell, thus gives rise to the

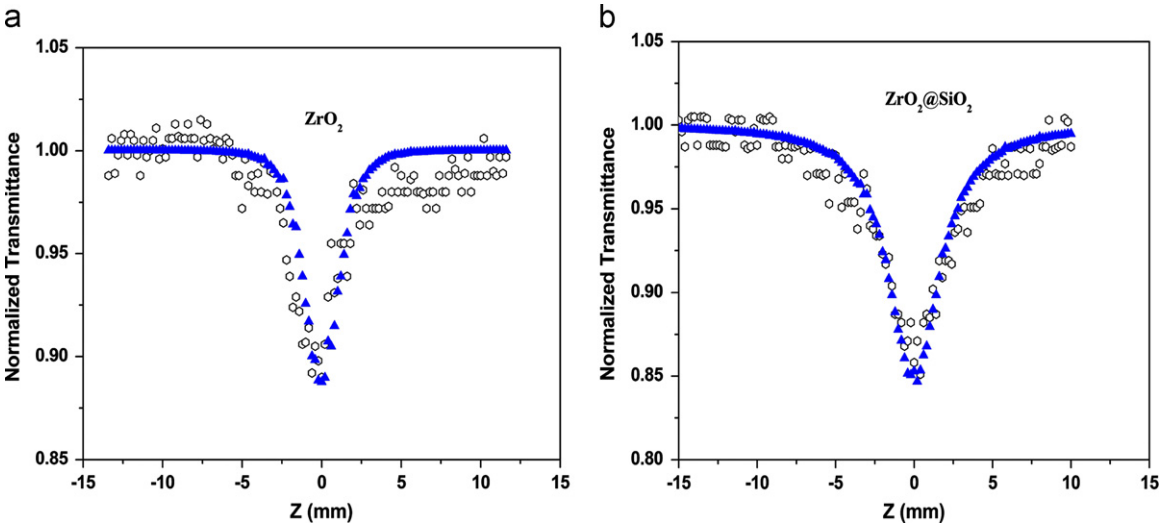

Fig. 8. Open aperture Z-scan curves of: (a) ZrO_2 and (b) ZrO_2@SiO_2 nanoparticles.

formation of trap states due to surface defects. When a photon of energy 2.33 eV is excited, the carriers may get excited to this defect level and free carrier absorption from these levels may occur with pulses of nanosecond duration which give rise to the large enhancement of the nonlinearity in the silica coated ZrO_2 nanoparticles.

4. Conclusion

Chemically synthesized ZrO_2 nanoparticles are coated with silica by Stober method. TEM and FT-IR results show that ZrO_2 nanoparticles are well covered with silica through Zr–O–Si chemical bonding. TGA and zeta potential studies reveal that silica coated nanoparticles have good thermal and dispersion stability compared to the bare ones. The average particle size of $ZrO_2@SiO_2$ nanoparticles was roughly calculated to about 35 nm. Optical nonlinearity measurements using nanosecond laser pulses at 532 nm reveal an effective 3 PA behavior at this wavelength. It is seen that the optical limiting performance is enhanced in core–shell nanoparticles. Both the samples exhibits high transmittance zones at longer wavelength apart from low cost and ease of preparation which of interest for optical limiting due to their better transparency to weak light.

Acknowledgments

The authors wish to thank Dr. Reji Philip of Raman Research Institute, Bangalore for providing NLO Lab facility.

References

[1] S. Somiya, N. Yamamoto, H. Yanagina, Science and Technology of Zirconia III, Advances in Ceramics, vol. 24A–24B, American Ceramic Society, Westerville, OH, 1988.
[2] G.Y. Liu, X.L. Yang, Y.M. Wang, Silica/poly(N,N′-methylenebisacrylamide) composite materials by encapsulation based on a hydrogen-bonding interaction, Polymer 48 (2007) 4385–4392.
[3] D.G. Yu, J.H. An, J.Y. Bae, S. Kim, Y.E. Lee, S.D. Ahn, S.Y. Kang, K.S. Suh, Carboxylic acid functional group containing inorganic core/polymer shell hybrid composite particles prepared by two-step dispersion polymerization, Colloids and Surfaces A: Physicochemical and Engineering Aspects 245 (2004) 29–34.
[4] Ahmed Mohamed El-Toni, Shu Yin, Tsugio Sato, Dense silica coating of titania nanoparticles by seeded polymerization technique, Colloids and Surfaces A: Physicochemical and Engineering Aspects 274 (2006) 229–233.
[5] W. Stober, A. Fink, E. Bohn, Controlled growth of monodisperse silica spheres in the micron size range, Journal of Colloid and Interface Science 26 (1968) 62–66.
[6] J.G. Yu, X.J. Zhao, J.C. Yu, G.R. Zhong, The grain size and surface hydroxyl content of super-hydrophilic TiO_2/SiO_2 composite nanometer thin films, Journal of Materials Science Letters 20 (2001) 1745–1748.
[7] Z. Dang, B.G. Anderson, Y. Amenomiya, B.A. Morrow, Silica-supported zirconia. 1. Characterization by infrared spectroscopy temperature-programmed desorption, and X-ray diffraction, Journal of Physical Chemistry 99 (1995) 14437–14443.
[8] J. Ho, M.K. Danquah, H. Wang, G.M. Forde, Protein loaded mesoporous silica spheres as a controlled delivery platform, Journal of Chemical Technology and Biotechnology 83 (2008) 351–358.
[9] B. Karthikeyan, J. Thomas, R. Kesavamoorthy, Optical limiting with off-resonant excitations in Ag nanocomposite glasses: a z-scan study, Journal of Non-Crystalline Solids 353 (2007) 1346–1349.
[10] B. Karthikeyan, M. Anija, Reji. Philip, In situ synthesis and nonlinear optical properties of Au:Ag nanocomposite polymer films, Applied Physics Letters 88 (2006) 053104–053106.